JACS
JOURNAL OF THE AMERICAN CHEMICAL SOCIETY
Article
pubs.acs.org/JACS

Kinetics of Nanoscale Self-Assembly Measured on Liquid Drops by Macroscopic Optical Tensiometry: From Mercury to Water and Fluorocarbons

Boris Haimov,[†,‡] Anton Iakovlev,[§] Rotem Glick-Carmi,[†] Leonid Bloch,[†] Benjamin B. Rich,[†] Marcus Müller,[§] and Boaz Pokroy*[,†,‡]

[†]Department of Materials Science and Engineering, Technion−Israel Institute of Technology, 32000 Haifa, Israel
[‡]Russell Berrie Nanotechnology Institute, Technion−Israel Institute of Technology, 32000 Haifa, Israel
[§]Institut für Theoretische Physik, Georg-August Universität, 37073 Göttingen, Germany

Supporting Information

ABSTRACT: Various molecules are known to form self-assembled monolayers (SAMs) on the surface of liquids. We present a simple method of investigating the kinetics of such SAM formation on sessile drops of various liquids such as mercury, water and fluorocarbon. To measure the surface tension of the drops we used an optical tensiometer that calculates the surface tension from the axisymmetric drop shape and the Young−Laplace relation. In addition, we estimated the SAM surface coverage fraction from the surface tension measured by other techniques. With this methodology we were able to optically detect concentrations as low as tenths of ppb increments of SAM molecules in solution and to compare the kinetics of SAM formation measured as a function of molecule concentration or chain length. The analysis is performed in detail for the case of alkanethiols on mercury and then shown to be more general by investigating the case of SAM formation of stearic acid on a water droplet in hexadecane and of perfluorooctanol on a Fluorinert FC-40 droplet in ethanol.

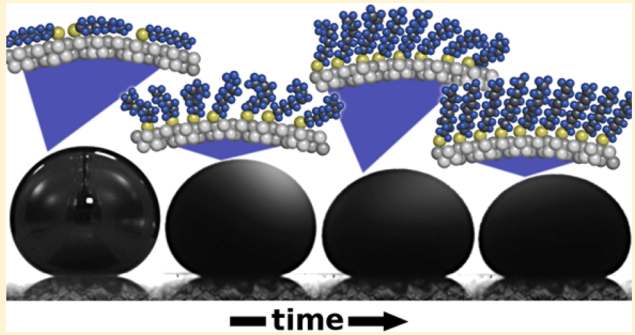

INTRODUCTION

Adsorption at interfaces has been studied for well over a century and is still the subject of substantial research. Adsorption is the process by which surfactant molecules bind to a surface while lowering its free energy.[1] Many types of interfaces can be created in this manner, depending on the surface material and the surfactant molecules.[2,3] The resulting interfaces may be divided into two main categories, multilayers and monolayers. The latter are usually termed self-assembled monolayers (SAMs).

Different types of SAMs organize themselves spontaneously from the gas or liquid phase on the surfaces of oxides, metals, and semiconductors into a two-dimensional (2D) semicrystalline phase. SAMs typically comprise a "headgroup" with specific surface-binding characteristics, alkyl spacer group and a "functional group", which determines the properties of the newly created, exposed surface once the monolayer is formed. For a given SAM headgroup it is possible to change the functional group, thereby tailoring the chemistry of the new surface formed.

The development of SAMs on surfaces has proved enormously useful in many areas of science and technology.[3] Among the most extensively studied and utilized SAMs are those of alkanethiols and (to a lesser extent) of disulfides.[4] These compounds bind strongly to coinage and noble metals such as gold,[4−6] silver,[7−9] copper,[10,11] platinum,[12,13] palladium,[14,15] and mercury.[16−18]

Beyond their basic research interest, SAMs have numerous applications, which are due to their ease of preparation that makes them especially suitable for the fabrication of nanostructured materials. Examples of potential applications of SAMs based on their interfacial characteristics are in wetting and wettability of surfaces,[19,20] sensing and sensors,[21,22] tribology,[23,24] organic electronics,[25,26] adhesion,[27,28] corrosion resistance,[29,30] nanofabrication,[31] and as templates for the nucleation and growth of crystals.[32−38]

The process of SAM formation on solid surfaces has also been intensively studied. This formation usually takes place via several steps:[2] Initially, the adsorption is driven by the diffusive transport of the SAM molecules in the bulk solution toward the surface. As a first stage the SAM-forming molecules become attached to the surface and lay flat on the substrate surface. Next, the adsorbed molecules group together via their attractive intermolecular van der Waals forces, forming small islands, which continue to grow toward each other until they become large enough to aggregate and eventually coalesce to form a

Received: September 21, 2015
Revised: October 6, 2015
Published: January 21, 2016

DOI: 10.1021/jacs.5b10446
J. Am. Chem. Soc. 2016, 138, 2585−2591

single, continuous SAM. The kinetics of such SAM formation have been studied mainly on solid metals, such as gold,[4,5,10,39−44] silver,[45−47] copper,[45] palladium,[15,48] platinum,[49] and other solids, using instruments, techniques or methodologies such as the quartz crystal microbalance (QCM), scanning tunneling microscopy (STM), infrared spectroscopy, optical ellipsometry, electrochemistry, and X-ray diffractometry (XRD).

Solid surfaces, in most cases, are not perfect and include structural defects such as grain boundaries, steps or cracks in crystalline planes. For instance, thin films formed via physical vapor deposition (PVD), exhibit particularly small grain sizes and concomitantly many grain boundaries. Surface roughness, which is often of the order of the SAM thickness, also hinders SAM quality. All these imperfections can be reduced by rather using liquid surfaces. Moreover the adsorption of SAMs and surfactants on liquids is very important both for fundamental studies as well as for various applications such as in the field of food and cosmetics technology (the stabilization of emulsions and foams).[50] There is also an interest in understanding various biological processes such as protein self-assembly and organization at interfaces as well as lipids.[51]

SAMs on liquid mercury have been used to study charge transport through the SAMs.[25,26] In those studies, the mercury drop serves as an electrode and the SAM is the nanometer-thick organic layer, through which electrons tunnel to the second electrode. As noted by Weiss et al. there are reproducibility issues in the field, partially due to the ordering of the SAM on the surface.[25] Adsorption of SAMs on liquid metal surfaces adds a dimension of freedom to that of adsorption processes on solid metal surfaces. This is because of the mobility of the liquid atoms, which (theoretically) allows for defect-free surfaces.

Here we show that we can study the kinetics of adsorption of various SAMs and surfactants on liquid droplets in real time. We have studied alkanthiol adsorption on liquid mercury, stearic acid on a water droplet in hexadecane and perfluorooctanol on a Fluorinert FC-40 droplet in ethanol. These three cases represent 3 major important general systems, namely liquid metals and reverse monolayers on oils or water.

While straightforward techniques are available for studying the kinetics of SAM formation on solids, this is a much more challenging task in the case of liquids. For solids, quartz microbalance (QCM) has been extensively used,[52] or surface plasmon resonance (SPR);[53] however, these methods are not suitable for liquids. In an attempt to overcome these problem-related liquid-surfaces, we exploited the phenomenon that the surface tension of hybrid organo-liquid surfaces (and thereby the liquid drop's shape) changes as surfactants adsorb on the drop's surface. Altering the surface tension of liquid metals (eutectic indium−gallium) as an example, has been found useful in reconfiguring, among other characteristics, the shape and flow of the droplets.[54−56] Unlike the case of solid substrates where the surface area remains constant, when SAMs form on the surface tension decreases, thereby changing the droplet area and promoting the formation of a new interface with environment. SAMs on liquid mercury[57−59] and various other liquids[60,61] have been studied in terms of their two-dimensional (2D) organization at or near equilibrium, mainly by means of X-ray diffraction and reflectivity techniques.

In our study we used liquids in the form of sessile droplets and studied the kinetics of the formation of various SAMs on their surfaces. For our experiment it is important to note that a liquid surface such as that of a sessile drop, which is flattened by gravity, allows the experimentalist to calculate the local surface tension from the local surface curvature and the difference in local pressures between the phases on each side of the interface.[62] The equation that relates to these quantities is known as the Young−Laplace equation, $\gamma = \Delta P/C$, where γ is the surface tension, ΔP is the pressure difference between the two phases at a given point on the interface, and C is the curvature of the given point on the interface. On the basis of this relation, commercial optical tensiometers allow fast calculation of the surface tension of a drop.

EXPERIMENTAL SECTION

Our experiments were performed in quartz cuvettes filled with a solvent and placed in an optical tensiometer as depicted in Figure S1 and Figure 1A. A small droplet of the desired liquid, 2.2 ± 0.1 μL, was placed at the bottom of the cuvette and its surface tension was calculated based on its shape, as described below. The surface tension of the sessile drop was always the highest and its shape the most spherical (see Figure 1B) prior to the injection of SAM molecules into the solution, as shown in see Figure 1A. The next step was to add the desired amount of SAM to the cuvette in order to reach its desired concentration within the cuvette.

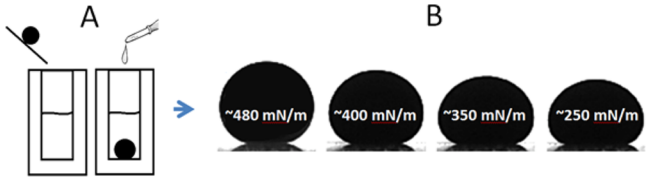

Figure 1. Kinetics of self-assembled monolayer (SAM) formation. (A) Experimental setup for placing a mercury droplet in the cuvette, for measurement by optical tensiometry. (B) Changing shape of mercury droplet during the decrease of surface tension owing to SAM formation. A drop with high surface tension is shown on the left and a drop with low surface tension on the right. (For details see Supporting Information.)

Before performing the time-dependent experiments in the presence of SAM molecules, it was important to verify that for a given sessile drop placed in the solvent in the absence of surfactants the measured surface tension and drop volume were constant over time. These control experiments, performed for all 3 systems studied herein, revealed very small fluctuations in surface tension over time as can be seen below in all the graphs presented in this paper. In addition performance of surface tension measurements for 10 different sessile drops over a period of 12 h, at a constant temperature of 30 °C in the absence of SAM molecules, confirmed that the surface tension measurements were indeed reliable and constant over time (see Figure S2). In this regard we have estimated the error (see error assessment in the Supporting Information). The error can in some cases be rather high (in the worst case up to a maximum of 25%) due mainly to vibrations, temperature instabilities and SAM molecule concentration gradients. We expect the error to be maximal in the initial stage because a lower surface tension leads to more pronounced deviations from a cap shape of the drop under gravity. Since we know that the initial surface tension of every sessile drop used is identical, we normalize all surface tensions in our analysis to the initial measured value of the surface tension.

Surface tension was measured with the Attension Theta Lite optical tensiometer (KSV NIMA Biolin Scientific). This instrument, which is based on a CCD camera connected to a computer, can be used to measure the surface tension, contact angle, drop volume, and some other relevant physical properties. From the digital images acquired with the CCD camera, the software deduces the surface tension and contact angle properties. The desired values are computed from the digital images by means of fitting algorithms. By using the Young−

DOI: 10.1021/jacs.5b10446
J. Am. Chem. Soc. 2016, 138, 2585−2591

Laplace equation that relates the drop shape of a given point on an interface to the local surface tension (γ), and by knowing the density difference between the drop material and solution ($\Delta\rho$), it is possible to deduce the surface tension of a given drop and by utilizing a simple axisymmetric fitting:[63]

$$\Delta P = (\Delta\rho)gz = \gamma\left(\frac{1}{R_1} + \frac{1}{R_2}\right)$$

where g is the gravitational acceleration, z, R_1 and R_2 are the vertical height and principal radii of the given point, respectively. The advantage of this technique compared to contact angle measurements consists in the absence of substrate effects. Moreover, the density of a sufficiently large droplet (larger than the capillary length) imparts a significant density contrast so that gravitation effects result in a visible deformation even at relatively small surfactant surface coverage. The surface tension is obtained by taking a snapshot of the drop, calculating from the image the local curvature of a given point on the interface, finding the local pressure difference at that given point on the interface, and using the Young−Laplace equation with gravitational flattening to calculate the surface tension at that given point.

RESULTS AND DISCUSSION

Time Resolved Decrease in Surface Tension. As a test study as described above, we used a tensiometer to first follow the changes in the surface tension over time of a mercury droplet caused by the adsorption of various alkanethiol SAMs onto it (see setup in Figure S1). Once the alkanethiol surfactants are added to the cuvette they immediately interact with the surface of the mercury drop and start forming a SAM on it, leading to a decrease in its surface tension. As the surface tension decreases, the shape of each droplet changes and gradually deviates from a nearly spherical cap shape and adopts a more ellipsoidal shape (Figure 1), because the decrease in surface tension results in the decrease in capillary length and increase in the effect of gravity. Figure 2 depicts a typical result of a complete experiment in which the surface tension is computed from the changing shape of the droplet until the second more slower stage of adsorption sets in.

In addition to this phenomenon observed on mercury we also studied the SAMs/surfactant adsorption on other liquids, e.g., on water and organic solvent droplets possessing considerably lower surface tensions. In the first case we studied the adsorption of saturated fatty acid (5 mM stearic acid) on the droplet of water placed in hexadecane solvent. Water and hexadecane are immiscible while stearic acid does dissolves in the latter but not in the former. We chose stearic acid as it is very common in nature and is widely used in detergents, soaps, various cosmetics and polymer softeners. A typical graph showing the decrease of the surface tension of water as a function of time due to the adsorption of stearic acid can be seen in Figure 2.

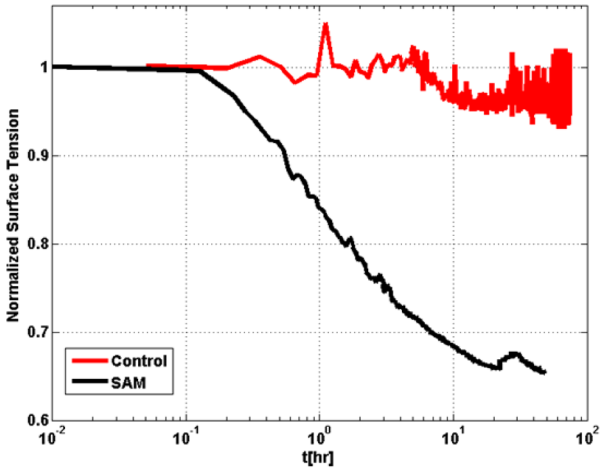

Figure 2. Kinetics of stearic acid (5 mM) SAM formation on water droplet. The plot shows the change in normalized surface tension as a function of time due to the adsorption of stearic acid (black line). The red line is a control experiment of a water droplet in hexadecane in the absence of the surfactant.

It is evident from Figure 2 that a similar behavior to that observed for the alkanethiol/mercury system can be observed. The main difference between these two systems is that the surface tension of mercury is much higher than that of water, which enhances the effect and that the SAM/liquid interaction is weaker. Nevertheless, in order to show that one can also use this methodology to study the adsorption of surfactants even on liquids with the lowest known surface tensions, we studied the adsorption of perfluorooctanol (CAS Number 647−42−7) on the surface of a droplet of Fluorinert FC-40 placed in ethanol. Fluorinert FC-40 has a surface tension as low as 16 mN/m. A typical graph showing the decrease of the Fluorinert surface tension as a function of time due to the adsorption of perfluorooctanol is presented in Figure 3. In both cases we also performed control experiments, in which we measured the time dependent surface tension of the droplets, however in the absence of the surfactant molecules. As can be clearly seen in both Figures 2 and 3 the time-dependent change in surface tension in the control experiments is negligible as compared to the effect of the adsorption.

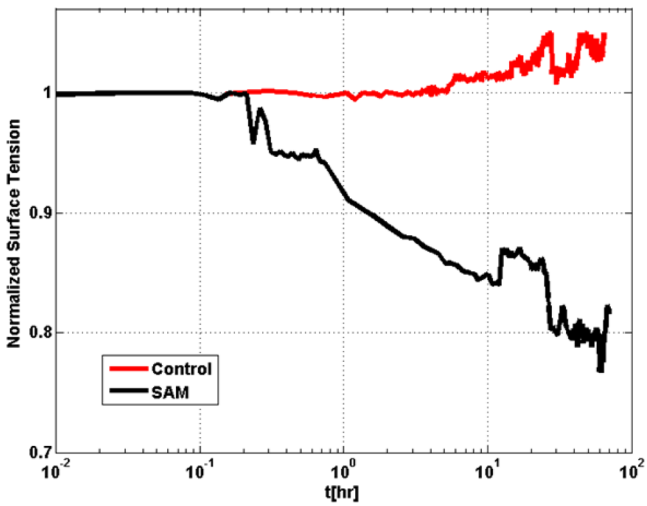

Figure 3. Kinetics of perfluorooctanol (5 mM) SAM formation on Fluorinert FC-40 droplet. The plot shows the change in normalized surface tension as a function of time due to the adsorption of perfluorooctanol (black line). The red line is a control experiment of a Fluorinert FC-40 droplet in ethanol in the absence of the surfactant.

Again, despite the low surface tension of the Fluorinert FC-40, it is very clear that one can indeed observe further decrease in the surface tension due to the surfactant adsorption.

In-Depth Study of the Alkanethiol/Mercury System: Effect of Chain Length. After showing that our method can probe the kinetics of formation of a variety of SAMs on various liquids we focus on one system more in depth. We chose here to perform this in-depth study on the alkanethiol/mercury

DOI: 10.1021/jacs.5b10446
J. Am. Chem. Soc. 2016, 138, 2585−2591

system and as a next step we wanted to determine how the chain length of the adsorbed alkanethiol SAM affects the kinetics of SAM formation. To this end we carried out a set of five experiments, each using one of the following five surfactants: $CH_3(CH_2)_7SH$ (octanethiol), $CH_3(CH_2)_9SH$ (decanethiol), $CH_3(CH_2)_{11}SH$ (dodecanethiol), $CH_3(CH_2)_{13}SH$ (tetradecanethiol) and $CH_3(CH_2)_{17}SH$ (octadecanethiol). In each experiment we maintained the SAM molecules at a constant concentration (1 mM) for about 12 h. The results in each case are depicted for a typical experiment in the plots in Figure 4, showing the surface tensions and the

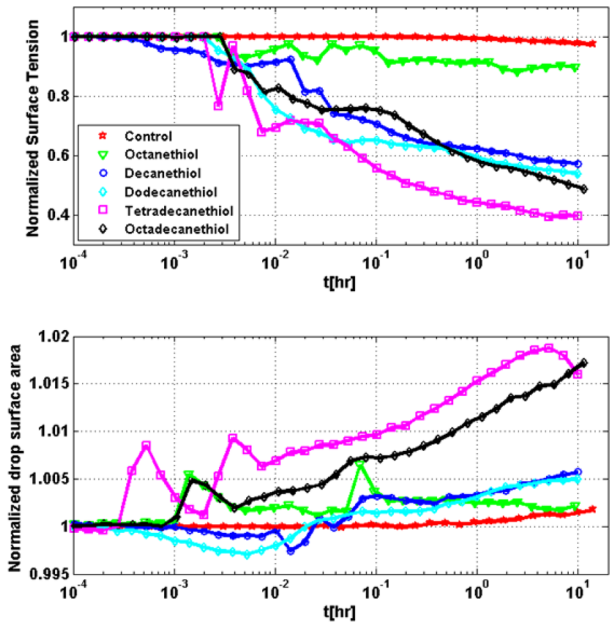

Figure 4. Kinetics of SAM formation and corresponding *n*-alkane-thiol surfactant chain lengths at a constant concentration of 1 mM. The uppermost plot shows the change in surface tension as a function of time and the lower plot shows the change in the total drop area as a function of time.

corresponding total areas of the drop that were measured by the optical tensiometer as described above. The total area of the drop is the sum of the area exposed to the SAM solution and the droplet-cuvette contact area not exposed to the SAM solution.

During the first few minutes of each experiment depicted in Figure 4, we see that the time taken for the initial kinetic change to occur was not constant, despite the fact that the surfactant was injected at almost the same moment in each case (at ±2 s). To determine the reason for this we performed 3 to 5 short-term experiments (each less than 1 min in duration) for each presented case. No constant representative time for the initial kinetic change was observed. During the first few seconds after the injection some optical distortions could be observed within the solution, temporarily affecting the measured shape of the sessile drop.

As shown in Figure 4 we could measure the changes in surface tension as a function of time, but we did not have information on the actual surface coverage of the SAMs on the droplet surface. Therefore, to correlate the changes in surface tension with the surface coverage we turned to the study by Kraack et al., who used X-ray diffraction to study the self-assembly of different alkanethiols on mercury at equilibrium (up to full coverage of the 2D crystalline organization).[64] For all alkanethiols up to and including octadecanethiol, those authors showed that for a coverage area of about 50 $Å^2$/molecule the surface pressure (i.e., the difference between the measured and the initial surface tension) was at most 50 mN/m. Therefore, to compare the kinetics of the different SAM molecules shown in Figure 2, we chose 50 $Å^2$/molecule as the reference coverage value and measured the time taken for each of the different SAMs to reach this value (which corresponds to a surface pressure of 50 mN/m). Table 1 shows the time (τ) needed for each specific SAM molecule to reach the surface area of 50$Å^2$/molecule or less, measured in terms of a surface pressure of 50 mN/m. We expect to find that the longer backbone of a SAM molecule corresponds to the faster SAM formation. This should be true, since longer adsorbate molecules interact stronger via van der Waals interactions with the surface of a respective droplet compared to their shorter counterparts. That is indeed what we observed, except in the case of tetradecanethiol, which demonstrated the fastest SAM formation time. One possible reason for the larger change in surface pressure in the case of longer-chain molecules might be that these molecules occupy a larger area on the droplet's surface at the initial adsorption stage, when the molecules are in "laying-down" conformation.

In regards to the reason why tetradecanethiol demonstrates the fastest SAM formation, our speculation is that this is the optimal length where (i) the van der Waals forces that constitute the thermodynamic driving force for SAM formation, increase with molecular weight of the SAM molecule and yet (ii) the kinetics become slow. In the initial and intermediate stages, the kinetics are dictated by the diffusion in solution whereas in the later stage, we expect that the kinetics are determined by the "tunneling" of the headgroup through the already partially formed SAM. Both kinetic factors become slower as we increase the length of the SAM molecule.

Effect of Concentration of SAM Molecules in the Solvent on the Kinetics of SAM Formation. To determine how the kinetics of the SAM formation process are affected by the initial concentration of SAM molecules within the solution, we repeated the time-dependent experiments but used different concentrations of SAM molecule. Figure 5 shows a representative plot depicting changes in kinetics with changes in concentration of the adsorbed species $CH_3(CH_2)_{11}SH$.

It is clear from the figure that the higher the initial SAM molecule concentration is, the higher SAM formation rate one obtains. We also observed that the higher the SAM concentration in the initial surfactant solution is, the greater change in the surface area of the drop one observes. Remarkably, although the lowest SAM concentration tested was as low as 10^{-7} M, a well-distinguished decrease in surface tension could still be observed. This clearly indicated that our sessile-drop procedure, although a macroscopic method, is very

Table 1. Time to 50 mN/m Surface Pressure for Different SAM Chain Lengths

SAM molecule	$CH_3(CH_2)_7SH$	$CH_3(CH_2)_9SH$	$CH_3(CH_2)_{11}SH$	$CH_3(CH_2)_{13}SH$	$CH_3(CH_2)_{17}SH$
τ [s]	9000	60	21	9	19

DOI: 10.1021/jacs.5b10446
J. Am. Chem. Soc. 2016, 138, 2585−2591

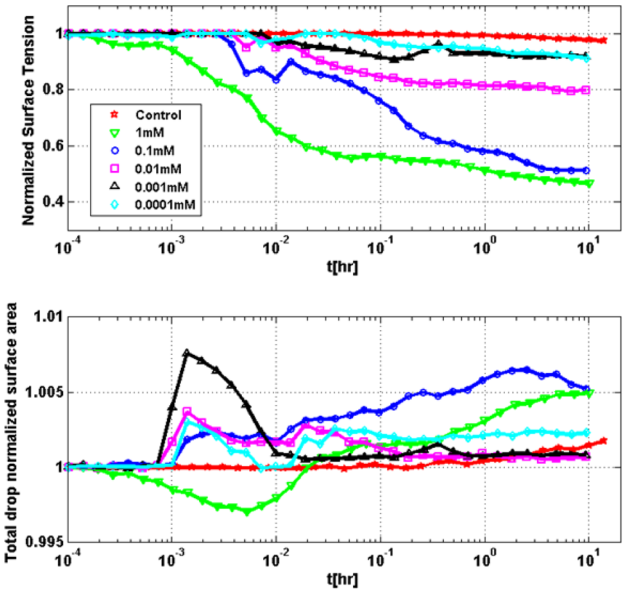

Figure 5. Kinetics of dodecanethiol SAM formation vs surfactant concentrations. The upper plot shows the change in surface tension as a function of time, and the lower plot shows the change in total drop area as a function of time.

sensitive to the adsorption of thiol molecules, so that concentrations as low as a few tenths of ppb of SAM molecules could be successfully detected even in the ethanolic solution. Moreover, detection occurred within a reasonable time period (a few hours).

Table 2. Summary of Formation Kinetics for Dodecanethiol SAM

dodecanethiol concentration [mM]	1	0.1	0.01	0.001	0.0001
τ [s]	4	15	67	230	6490

Table 2 presents a summary of the time (τ) required to achieve an occupation of 50 Å^2/molecule, for varying concentrations of dodecanethiol. Use of the corresponding surface pressure of 50 mN/m as a reference posed a problem for the very low concentrations (0.001 mM and 0.0001 mM). For these concentrations the surface pressure did not reach 50 mN/m, and we therefore had to use a lower surface pressure value to perform qualitative comparisons. Referring again to ref 64, we noted that in the specific case of the dodecanethiol molecules it is enough to work with a surface pressure of 30 mN/m in order to achieve surface occupation of 50 Å^2/molecule.

Since no theoretical model yet exists that can fully and accurately describe the adsorption of SAMs on liquid metal surfaces, we focused on a representative SAM molecule and tried to fit it to some relevant adsorption models. The case of 1 mM dodecanethiol was chosen for this purpose, because its samples were the least noisy among all the experiments we conducted. To fit the experimental data we used the Volmer isotherm[65]

$$\gamma_0 - \gamma \equiv \pi = \frac{kTN}{A - A_1} = \frac{kT\sigma}{1 - a_1\sigma}$$

or, in terms of the dimensionless coverage:

$$\pi = \frac{kT\sigma_{max}\theta}{1 - a_1\sigma_{max}\theta}$$

where γ_0 is the initial surface tension, γ is the surface tension for a given surface coverage $\sigma = N/A$, with A and A_1 being the total area and the total excluded area of mercury droplet and surfactant, respectively; a_1 is the excluded area per molecule and σ_{max} is the largest possible value of coverage in laying-down conformations.

Langmuir Adsorption. SAM adsorption can be described in terms of the well-known Langmuir model:[66]

$$\theta(t) = 1 - e^{-r(t-t_0)}$$

where t_0 accounts for the initial time shift in the experimental measurements and r is the reaction rate of the adsoption. Plugging this into the Volmer isotherm we derive a surface pressure π_L for the Langmuir model:

$$\pi_L = \frac{kT\sigma_{max}(1 - e^{-r(t-t_0)})}{1 - a_1\sigma_{max}(1 - e^{-r(t-t_0)})}$$

The fit of our experimental measurements by the above equation is shown in Figure 6. The fitting parameters are $kT\sigma_{max} = 0.0333$ eV/Å^2, $a_1\sigma_{max} = -1.284$, and $r = 0.0243$ s^{-1}, which provides the time constant $1/r = 41.22$ s. Measurements were carried out at $T = 303$ K, which yields $1/\sigma_{max} = 0.78$ Å^2 and $a_1 = -1.006$ Å^2.

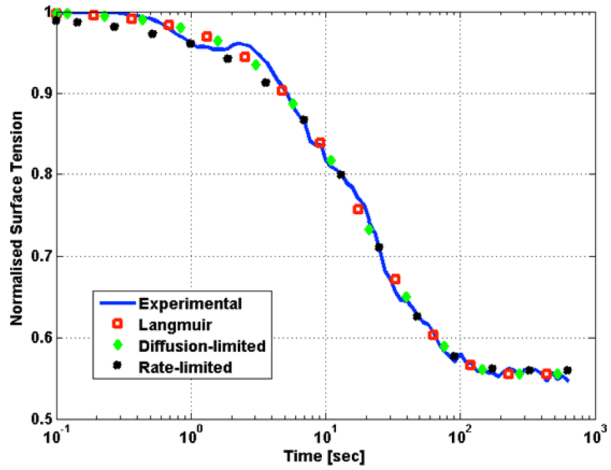

Figure 6. Dodecanethiol fittings with kinetics isotherm: Langmuir (red squares), diffusion-limited Langmuir (green diamonds), rate-limited (black stars) and experimental results (blue circles).

Diffusion-Limited Langmuir Adsorption. In diffusion-limited adsorption, timing of the adsorption process is dictated by the diffusion rate of the adsorbed species within the solution. In this case it was assumed that diffusion is the slowest of all the processes taking place during the adsorption procedure. In such a case, the coverage is defined as[66]

$$\theta(t) = 1 - e^{-r\sqrt{t-t_0}}$$

In this case we have the surface pressure π_{DLL} given by

$$\pi_{DLL} = \frac{kT\sigma_{max}(1 - e^{-r\sqrt{t-t_0}})}{1 - a_1\sigma_{max}(1 - e^{-r\sqrt{t-t_0}})}$$

DOI: 10.1021/jacs.5b10446
J. Am. Chem. Soc. 2016, 138, 2585−2591

with the fitting parameters $kT\sigma_{max} = 0.002$ eV/Å^2, $a_1\sigma_{max} = 0.86$, $r = 0.54$ s$^{-1/2}$, yielding $1/\sigma_{max} = 12.5$ Å^2, $a_1 = 10.75$ Å^2, and $1/r = 1.85$ s$^{1/2}$. The diffusion coefficients (D) can be estimated as follows:[67]

$$D = \frac{r^2 \pi \sigma_{max}^2}{4C_0}$$

where C_0 is the initial bulk concentration of the adsorbed species. For $C_0 = 1$ mM we obtain $D = 4.14 \times 10^{-7}$ cm^2/s, which is of the typical order of magnitude for the alkanethiol systems.[68]

Rate-Limited Adsorption. We can also consider a scenario of desorption via a simple multistage process in which the molecules are first adsorbed onto the surface in a weakly bound state from which they can either desorb back into the solution or, at a later stage, bind more strongly to the surface. In this case the coverage is given by[66]

$$\theta(t) = \frac{e^{r'(t-t_0)} - 1}{e^{r'(t-t_0)} + k_E}$$

where $r' = (1 + k_E)r$ and k_E accounts for the adsorption onto the precursor state.

In this case, the surface pressure π_{RL} is given by

$$\pi_{RL} = \frac{kT\sigma_{max}\left(\frac{e^{r'(t-t_0)} - 1}{e^{r'(t-t_0)} + k_E}\right)}{1 - a_1\sigma_{max}\left(\frac{e^{r'(t-t_0)} - 1}{e^{r'(t-t_0)} + k_E}\right)}$$

The results of the respective fitting are shown in Figure 6. The fitting parameters are $kT\sigma_{max} = 0.017$ eV/Å^2, $a_1\sigma_{max} = -0.18$, $k_E = -0.48$, and $r' = 0.0243$ s^{-1}, yielding $1/\sigma_{max} = 1.54$ Å^2, $a_1 = -0.28$ Å^2, and $1/r = 41.15$ s.

From the three fittings assessed and presented above, it can be seen that some of the fitting parameters for the Langmuir and the rate-limited models acquire negative values. This suggests that neither the Langmuir nor the rate-limited adsorption can describe the adsorption process in our experiments. Thus, of the three models tested in this work, the one that best describes the experimental results is the diffusion-limited Langmuir model.

CONCLUSIONS

In this work we have shown that the kinetics of various SAM formation can be investigated by a relatively simple method, in which a sessile drop is measured by optical tensiometry. In this procedure, probing on the macro scale yields information on the subnanometer scale. Using this setup we were able to detect the adsorption of surfactant molecules on short (minutes) as well as on large (hours) time scales for the concentrations of SAM molecules in solution, as low as a few tenths of ppb. As the result we could quantify the kinetics of SAM formation as a function of different linear alkanethiol concentrations and different backbone lengths on a liquid mercury drop. We also demonstrated that we were able to detect the adsorption kinetics for other systems such as fatty acid on water and perfluorooctanol on a fluorinated carbon liquid. The results for the latter liquid with one of the lowest surface tensions known prove that our method is universal and suitable for studying the kinetics of adsorption even for the systems that feature very small reduction of the surface pressure in the course of adsorption. To the best of our knowledge this is the first study in which the kinetics of the SAM formation on liquid mercury has been systematically investigated in situ. Examination of the relationship between the kinetics of SAM formation and the backbone length of SAM molecules revealed, in general, that the longer the chain the faster the formation of the SAM. Examination of the relationship between the kinetics of SAM formation and the concentration of SAM molecule demonstrates that the higher the molecular concentration the faster the SAM formation. Our results point to the diffusion of thiols toward the liquid surface, and their subsequent chemical adsorption, as the main mechanism of adsorption for the studied systems.

In the specific case of Mercury/thiols, we also showed that in most of the experiments conducted with a SAM molecular concentration of 1 mM, the surface coverage had already reached 50 Å^2/molecule within the first few minutes of the experiment. Although the surface excess usually increases during adsorption of molecules on solid surface, when molecules are adsorbed on liquid surfaces the surface excess might, in principle, decrease. This is because, in contrast to solids, during adsorption on liquids the surface area of the liquid increases.

We have no doubt that the method and procedure we used herein can yield exciting results in many other systems in which a surfactant adsorbs on the surface of various liquids and yield valuable insights even on biologically relevant questions.

ASSOCIATED CONTENT

Supporting Information

The Supporting Information is available free of charge on the ACS Publications website at DOI: 10.1021/jacs.5b10446.

Details of experimental setup, error assessment and kinetics of SAM formation of alkanethiols with odd chain lengths, including Figures S1−S3. (PDF)

AUTHOR INFORMATION

Corresponding Author

*bpokroy@tx.technion.ac.il

Notes

The authors declare no competing financial interest.

ACKNOWLEDGMENTS

This joint research project was financially supported by the state of Lower-Saxony and the Volkswagen Foundation, Hannover, Germany, grant number ZN2726. AI and MM thank D. Bedrov for stimulating discussions.

REFERENCES

(1) Adamson, A. W.; Gast, A. P. *Physical Chemistry of Surfaces*, 6th ed.; Wiley-Interscience: New York, 1987.
(2) Schwartz, D. K. *Annu. Rev. Phys. Chem.* **2001**, *52*, 107.
(3) Love, J. C.; Estroff, L. A.; Kriebel, J. K.; Nuzzo, R. G.; Whitesides, G. M. *Chem. Rev.* **2005**, *105*, 1103.
(4) Nuzzo, R. G.; Allara, D. L. *J. Am. Chem. Soc.* **1983**, *105*, 4481.
(5) Poirier, G. E.; Pylant, E. D. *Science* **1996**, *272*, 1145.
(6) Evans, S. D.; Freeman, T. L.; Flynn, T. M.; Batchelder, D. N.; Ulman, A. *Thin Solid Films* **1994**, *244*, 778.
(7) Walczak, M. M.; Chung, C. K.; Stole, S. M.; Widrig, C. A.; Porter, M. D. *J. Am. Chem. Soc.* **1991**, *113*, 2370.
(8) Fenter, P.; Eisenberger, P.; Li, J.; Camillone, N.; Bernasek, S.; Scoles, G.; Ramanarayanan, T. A.; Liang, K. S. *Langmuir* **1991**, *7*, 2013.
(9) Fenter, P.; Gustafsson, T. *Phys. Rev. B: Condens. Matter Mater. Phys.* **1991**, *43*, 12195.

DOI: 10.1021/jacs.5b10446
J. Am. Chem. Soc. 2016, 138, 2585−2591

(10) Laibinis, P. E.; Whitesides, G. M.; Allara, D. L.; Tao, Y. T.; Parikh, A. N.; Nuzzo, R. G. *J. Am. Chem. Soc.* **1991**, *113*, 7152.
(11) Herdt, G. C.; King, D. E.; Czanderna, A. W. *Z. Phys. Chem.* **1997**, *202*, 163.
(12) Lee, T. R.; Laibinis, P. E.; Folkers, J. P.; Whitesides, G. M. *Pure Appl. Chem.* **1991**, *63*, 821.
(13) Lang, P.; Mekhalif, Z.; Rat, B.; Garnier, F. *J. Electroanal. Chem.* **1998**, *441*, 83.
(14) Love, J. C.; Wolfe, D. B.; Chabinyc, M. L.; Paul, K. E.; Whitesides, G. M. *J. Am. Chem. Soc.* **2002**, *124*, 1576.
(15) Carvalho, A.; Geissler, M.; Schmid, H.; Michel, B.; Delamarche, E. *Langmuir* **2002**, *18*, 2406.
(16) Magnussen, O. M.; Ocko, B. M.; Deutsch, M.; Regan, M. J.; Pershan, P. S.; Abernathy, D.; Grubel, G.; Legrand, J. F. *Nature* **1996**, *384*, 250.
(17) Muskal, N.; Mandler, D. *Electrochim. Acta* **1999**, *45*, 537.
(18) Pokroy, B.; Aichmayer, B.; Schenk, A. S.; Haimov, B.; Kang, S. H.; Fratzl, P.; Aizenberg, J. *J. Am. Chem. Soc.* **2010**, *132*, 14355.
(19) Wenzl, I.; Yam, C. M.; Barriet, D.; Lee, T. R. *Langmuir* **2003**, *19*, 10217.
(20) Colorado, R.; Lee, T. R. *Langmuir* **2003**, *19*, 3288.
(21) Butt, H. J. *J. Colloid Interface Sci.* **1996**, *180*, 251.
(22) Berger, R.; Delamarche, E.; Lang, H. P.; Gerber, C.; Gimzewski, J. K.; Meyer, E.; Guntherodt, H. J. *Science* **1997**, *276*, 2021.
(23) Leggett, G. J. *Anal. Chim. Acta* **2003**, *479*, 17.
(24) Moser, A. E.; Eckhardt, C. J. *Thin Solid Films* **2001**, *382*, 202.
(25) Weiss, E. A.; Kriebel, J. K.; Rampi, M. A.; Whitesides, G. M. *Philos. Trans. R. Soc., A* **2007**, *365*, 1509.
(26) Fan, F. R. F.; Yang, J. P.; Cai, L. T.; Price, D. W.; Dirk, S. M.; Kosynkin, D. V.; Yao, Y. X.; Rawlett, A. M.; Tour, J. M.; Bard, A. J. *J. Am. Chem. Soc.* **2002**, *124*, 5550.
(27) Houston, J. E.; Kim, H. I. *Acc. Chem. Res.* **2002**, *35*, 547.
(28) Petrenko, V. F.; Peng, S. *Can. J. Phys.* **2003**, *81*, 387.
(29) Burleigh, T. D.; Gu, Y.; Donahey, G.; Vida, M.; Waldeck, D. H. *Corrosion* **2001**, *57*, 1066.
(30) Jennings, G. K.; Yong, T. H.; Munro, J. C.; Laibinis, P. E. *J. Am. Chem. Soc.* **2003**, *125*, 2950.
(31) Kim, E.; Kumar, A.; Whitesides, G. M. *J. Electrochem. Soc.* **1995**, *142*, 628.
(32) Flath, J.; Meldrum, F. C.; Knoll, W. *Thin Solid Films* **1998**, *329*, 506.
(33) Meldrum, F. C.; Flath, J.; Knoll, W. *J. Mater. Chem.* **1999**, *9*, 711.
(34) Heywood, B. R.; Mann, S. *Adv. Mater.* **1994**, *6*, 9.
(35) Aizenberg, J.; Black, A. J.; Whitesides, G. H. *J. Am. Chem. Soc.* **1999**, *121*, 4500.
(36) Aizenberg, J.; Black, A. J.; Whitesides, G. M. *Nature* **1999**, *398*, 495.
(37) Han, Y. J.; Aizenberg, J. *Angew. Chem., Int. Ed.* **2003**, *42*, 3668.
(38) Pokroy, B.; Chernow, V. F.; Aizenberg, J. *Langmuir* **2009**, *25*, 14002.
(39) Porter, M. D.; Bright, T. B.; Allara, D. L.; Chidsey, C. E. *J. Am. Chem. Soc.* **1987**, *109*, 3559.
(40) Dubois, L. H.; Nuzzo, R. G. *Annu. Rev. Phys. Chem.* **1992**, *43*, 437.
(41) Bain, C. D.; Whitesides, G. M. *Science* **1988**, *240*, 62.
(42) Bain, C. D.; Evall, J.; Whitesides, G. M. *J. Am. Chem. Soc.* **1989**, *111*, 7155.
(43) Biebuyck, H. A.; Bain, C. D.; Whitesides, G. M. *Langmuir* **1994**, *10*, 1825.
(44) Dubois, L. H.; Zegarski, B. R.; Nuzzo, R. G. *J. Chem. Phys.* **1993**, *98*, 678.
(45) Laibinis, P. E.; Whitesides, G. M.; Allara, D. L.; Tao, Y. T.; Parikh, A. N.; Nuzzo, R. G. *J. Am. Chem. Soc.* **1991**, *113*, 7152.
(46) Walczak, M. M.; Chung, C.; Stole, S. M.; Widrig, C. A.; Porter, M. D. *J. Am. Chem. Soc.* **1991**, *113*, 2370.
(47) Fenter, P.; Eisenberger, P.; Li, J.; Camillone, N., III; Bernasek, S.; Scoles, G.; Ramanarayanan, T.; Liang, K. *Langmuir* **1991**, *7*, 2013.
(48) Love, J. C.; Wolfe, D. B.; Haasch, R.; Chabinyc, M. L.; Paul, K. E.; Whitesides, G. M.; Nuzzo, R. G. *J. Am. Chem. Soc.* **2003**, *125*, 2597.
(49) Li, Z.; Chang, S.-C.; Williams, R. S. *Langmuir* **2003**, *19*, 6744.
(50) Dickinson, E. *Colloids Surf., B* **1999**, *12*, 105.
(51) Stottrup, B. L.; Veatch, S. L.; Keller, S. L. *Biophys. J.* **2004**, *86*, 2942.
(52) Karpovich, D. S.; Blanchard, G. J. *Langmuir* **1994**, *10*, 3315.
(53) Peterlinz, K. A.; Georgiadis, R. *Langmuir* **1996**, *12*, 4731.
(54) Wang, M.; Trlica, C.; Khan, M. R.; Dickey, M. D.; Adams, J. J. *J. Appl. Phys.* **2015**, *117*, 117.
(55) Khan, M. R.; Trlica, C.; Dickey, M. D. *Adv. Funct. Mater.* **2015**, *25*, 671.
(56) Khan, M. R.; Trlica, C.; So, J. H.; Valeri, M.; Dickey, M. D. *ACS Appl. Mater. Interfaces* **2014**, *6*, 22467.
(57) Deutsch, M.; Magnussen, O.; Ocko, B.; Regan, M.; Pershan, P. *Thin Films* **1998**, *24*, 180.
(58) Ocko, B.; Kraack, H.; Pershan, P. S.; Sloutskin, E.; Tamam, L.; Deutsch, M. *Phys. Rev. Lett.* **2005**, *94*, 017802.
(59) Magnussen, O. M.; Ocko, B. M.; Deutsch, M.; Regan, M. J.; Pershan, P. S.; Abernathy, D.; Grübel, G.; Legrand, J.-F. *Nature* **1996**, *384*, 250.
(60) Zhang, Z. J.; Mitrinovic, D. M.; Williams, S. M.; Huang, Z. Q.; Schlossman, M. L. *J. Chem. Phys.* **1999**, *110*, 7421.
(61) Tikhonov, A. M.; Li, M.; Schlossman, M. L. *J. Phys. Chem. B* **2001**, *105*, 8065.
(62) De Gennes, P.-G. *Rev. Mod. Phys.* **1985**, *57*, 827.
(63) Rotenberg, Y.; Boruvka, L.; Neumann, A. W. *J. Colloid Interface Sci.* **1983**, *93*, 169.
(64) Kraack, H.; Tamam, L.; Sloutskin, E.; Deutsch, M.; Ocko, B. *Langmuir* **2007**, *23*, 7571.
(65) Ruthven, D. M. *Principles of adsorption and adsorption processes*; John Wiley & Sons: 1984; p 68.
(66) Dannenberger, O.; Buck, M.; Grunze, M. *J. Phys. Chem. B* **1999**, *103*, 2202.
(67) Rahn, J.; Hallock, R. *Langmuir* **1995**, *11*, 650.
(68) Balmer, T. E.; Schmid, H.; Stutz, R.; Delamarche, E.; Michel, B.; Spencer, N. D.; Wolf, H. *Langmuir* **2005**, *21*, 622.

DOI: 10.1021/jacs.5b10446
J. Am. Chem. Soc. 2016, 138, 2585−2591